Asymmetrical Modulation Strategies for Partially Covered Inductors in Flexible Induction Heating Appliances

Pablo Guillen, Héctor Sarnago, *Senior Member*, *IEEE*, Óscar Lucía, *Senior Member*, *IEEE*, and José Miguel Burdío, *Senior Member*, *IEEE*.
Department of Electronic Engineering and Communications, I3A
Universidad de Zaragoza
Zaragoza, Spain
pguillenm@unizar.es

***Abstract*—Cost-effective multi-output resonant inverter topologies are a key enabling technology for the development of flexible surfaces for induction heating appliances. These topologies present several challenges when applied to a wide range of IH-loads simultaneously. In this paper, two asymmetrical modulations are proposed as an alternative solution to control output power. The proposed approach has been verified using an experimental prototype featuring 2 induction heating loads up to 3.6 kW with output power control in the whole operating range.**

Keywords—Asymmetrical modulation, Power control, Home Appliances, Induction Heating

I. Introduction

Induction heating (IH) is the base technology for a wide range of industrial, domestic, and biomedical applications [1]. In the domestic area, these systems exhibit remarkable advantages in terms of efficiency, safety, cleanliness, and fast heating that has allowed this technology to become the leading one in the last decade.

In this context, design tendencies on induction heating appliances are leading towards more flexible surfaces [2] with the purpose of improving the user experience. This increase of flexibility allows the use of a variable number of pots independently of their shape or size over the cooktop, being the inductor activation selected by the device (Fig. 1) [3].

In order to design and implement such systems, several challenges have to be faced, being the most relevant ones: The design of small inductors with low mutual coupling [4-6], the development of multi-output power converters [7-10], and the control of a high number of loads [11-14]. Those challenges have to be solved reaching a balance between complexity, cost, and performance.

Inductor distribution on flexible surfaces is designed to reach a wide range of pot positions, fulfilling, at least, all the classical hob positions. However, the absence of restrictions for positioning prevents the final user from being aware of optimum positions for increased inductor coverage. This leads to partially covered inductors with different coupling between the inductor and the pot and, consequently, different supplied power, which leads to an uneven heating of the pan.

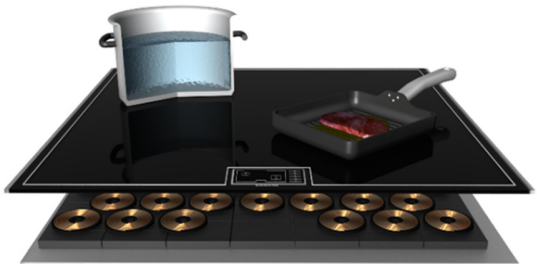

Fig. 1. *Flexible induction heating surface.*

In this paper, asymmetrical modulation strategies are presented in order to achieve an efficient and highly independent power control over partially covered inductors allowing an even heating of the pan and ensuring the proper converter operation. The remainder of this paper is organized as follows: In Section II, the previously discussed challenge is deeply described for a given topology. Section III presents the proposed control strategies and analyze them. Section IV shows the experimental results used to validate the proposals. Finally, the conclusions of this paper are drawn in Section V.

II. Series Resonant Multi-inverter Power Control

A multi-output implementation based on the series-resonant half-bridge inverter can be seen in Fig. 2 [15]. It is composed of a full-bridge diode rectifier that supplies bus voltage, v_b, to several inverters. Each of the half-bridge inverters are composed of the power devices, transistors with antiparallel diode, and a snubber capacitor to reduce switching losses. Each IH load, is modelled by its equivalent series inductance, L_r, and resistance, R_L, whose values change with the pot material, inductor-pot coupling, switching frequency [16] or temperature, among others. To complete the resonant tank, a capacitor is connected in series. Typically, this capacitor is split in order to improve high frequency harmonic behavior.

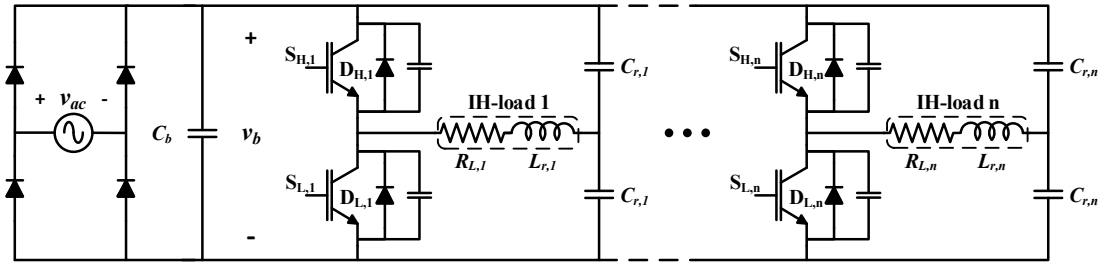

Fig. 2. *Proposed topology.*

TABLE I. RESONANT LOAD PARAMETERS AT RESONANT FREQUENCY

	Inductor coverage		
	100%	***75%***	***50%***
R_L	4.11 Ω	3.87 Ω	2.99 Ω
L_r	86 µH	83 µH	78 µH
Cr	220 nF		

This topology allows an almost independent power supply to all the loads while avoiding problems such as single inverter multiple outputs or power routing, and therefore helps to analyze the topology practical limits by decoupling problems.

As it has been previously discussed, the equivalent IH load depends on various parameters, being the pot-inductor coupling the most relevant, and therefore for a given geometry and a certain pot the relative position between them. Partially covered inductors present critical handicaps for the correct cooktop behavior. The first one, and the most relevant one for a good user experience, is the reduced overlapping area between the pot and the inductor, which is roughly the area where the heat is generated. Secondly, coupling variation implies equivalent resistance and inductance variations that may result in increased currents through the load and power devices. As a representative example, TABLE I shows the IH load parameter variations with the inductor coverage percentage.

A. Classical Modulation Strategies

Typically, half-bridge inverters for induction heating are controlled by using a strategy of variable frequency, f_{sw}, and duty cycle, D, by its acronym VFDC [17]. This strategy normally relies on a zero voltage switching (ZVS) operation in order to improve the efficiency. Consequently, this topology presents several restrictions in the operational frequency range. Firstly, to achieve ZVS, the switching frequency has to be over the resonant frequency. Secondly, due to the shared bus, switching frequencies are limited in order to avoid generating acoustic noise or, in other words, inverters have to share the same frequencies or space them in bands greater than 20 kHz to avoid intermodulation noise.

In addition, due to the use of snubber capacitors, the turn-off current has to be high enough for the proper charge and discharge these capacitors, generating an additional constraint, not only on the f_{sw}, but also on the duty cycle.

Considering the parameters shown in TABLE I, the proposed topology has been simulated so that output power, P_o,

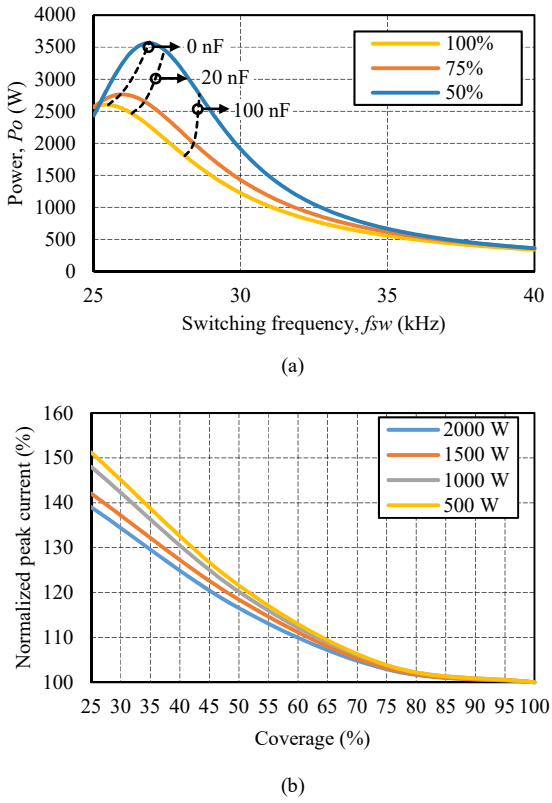

Fig. 3. *Load power as a function of frequency for different inductor coverages (a). The chart displays proper ZVS switching for different snubber capacitances. Normalized peak current as a percentage of the 100% covered inductor current for different power levels (b).*

and load current, i_o, variation with different inductor-pot coverage ratios can be seen.

For those simulations several snubber capacitances are simulated in order to show the proper operation areas. As it can be seen, coverage reduction implies an equivalent inductance variation and therefore a resonant frequency displacement to higher frequencies. Thus, in Fig. 3 (a) can be seen that power levels for a given switching frequency, f_{sw}, do not vary proportional to the inductor-pot overlapping area, but they increase. This generates an "edge heating" effect in the IH load that creates a considerable temperature gradient on the pan that may even damage it. Also, due to the equivalent resistance reduction and resonant frequency variation, the current trough the load increases for the same power (Fig. 3 (b)). This current

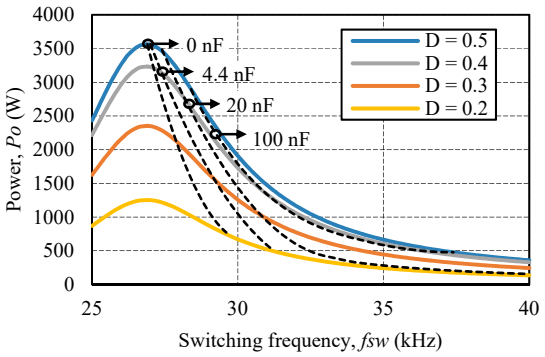

Fig. 4. *Load power as a function of frequency for different duty cycles and proper ZVS switching areas for different snubber capacitances.*

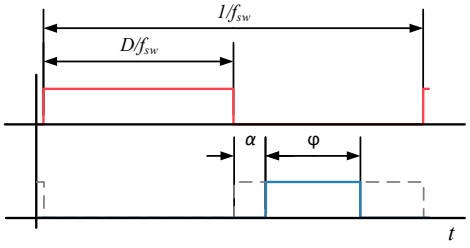

Fig. 5. *Asymmetrical conduction mode control parameters.*

has to be controlled in order to guarantee components safe operation.

Considering these restrictions, the more straightforward power control option is based on duty cycle control. In Fig. 4, the power curves for various duty cycles can be seen. The proper ZVS operation range is also showed with and without snubber capacitances. As it can be seen some restriction appear over proper power delivery.

To overcome this limitation, snubber capacitance may be reduced or eliminated, however this would result in high commutation losses. Therefore, alternative modulations would be presented for the case of no snubber capacitors.

III. Proposed Asymmetrical Modulations

Asymmetrical conduction mode operation occurs when an uneven transistor activation is performed. Therefore, by reducing one of the transistors activation time, the applied rms voltage is reduced, and therefore, the output power is decreased. This way it is possible to decrease the output power without varying the switching frequency.

In the presented case, and in contrast with duty variation, asymmetrical conduction mode is reached by modifying only the low transistor activation parameters as is shown in Fig. 5. However, in order to increase efficiency, f_{sw} should be close to resonant frequency while the upper transistor duty cycle remains fixed at 50%.

Moreover, to achieve the required output power for each load, f_{sw} has to be chosen so that the output power is the required or higher for each load. This way the reached power could be

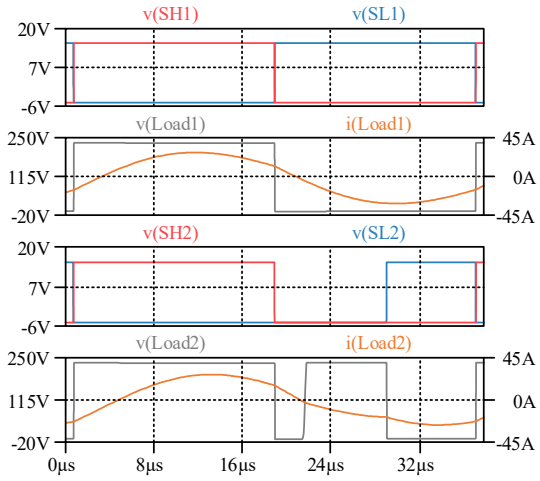

Fig. 6. *Non-complementary pulse delay control (NC PDC) simulation, α=100°. 2000 W for a 100% covered inductor (IH-load 1) and 1000 W for a 50% covered one (IH-load 2).*

diminished by means of the asymmetrical conduction modulation.

Two asymmetrical modulations are analyzed, simulated, and experimentally verified. The first one is based on the variation of the activation angle, α, whereas, the second one, is based on the variation of the active time, φ.

A. Non-complementary pulse delay control

In the case of non-complementary pulse delay control (NC PDC), based on α variation, when the current through the low side antiparallel diode, D_L, reaches zero conduction starts in the high side antiparallel diode, D_H. Thus, in order to ensure asymmetrical conduction mode, α is to be greater than the low side diode, D_L, conduction time. If the activation angle is not big enough, no reduction in the output power occurs.

Once S_L is turned on, current flows through it until it is turned off and then current flows through D_H and S_H consecutively. When S_H is turned off current flows through D_L until it crosses zero and D_H is activated. If the time until S_L is long enough, and due to the resonant characteristics of the load, the current through D_H would reach zero again and D_L would be activated and so on.

The simulated waveforms for 2000 W for a 100% covered inductor and the proportional power level for a 50% covered one can be seen in Fig. 6.

It can be seen that α variation implies a hard-switching turn-on sequence on the low side transistor which increases power losses and therefore a reduced efficiency. However, this asymmetrical strategy ensures ZVS commutation in S_H.

B. Non-complementary pulse width modulation

In the case of non-complementary pulse width modulation (NC PWM), based on φ variation, the reduction of S_L conduction time, means an increase of D_H conduction time. For this case, for a high φ parameter power reduction is similar to the achieved by means of duty cycle variation. However, when current

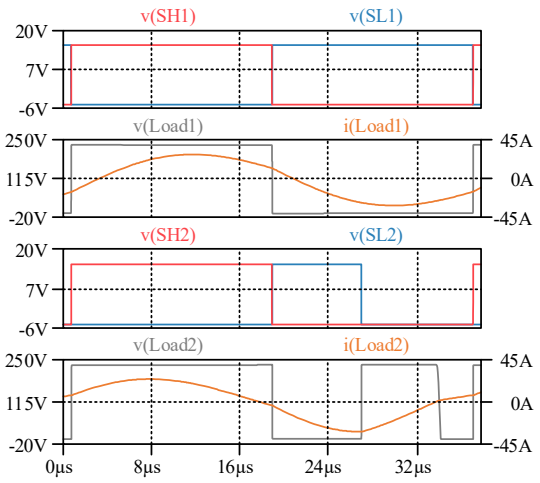

Fig. 7. *Non-complementary pulse width modulation (NC PWM) simulation, φ=80°. 2000 W for a 100% covered inductor (IH-load 1) and 1000 W for a 50% covered one (IH-load 2).*

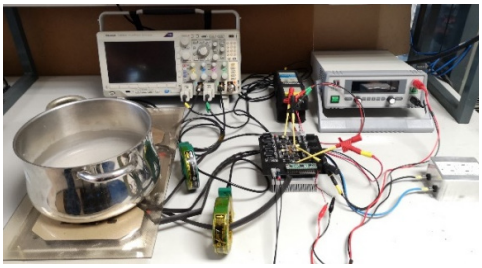

Fig. 8. *Experimental setup composed by two half-bridge inverters connected to the same bus voltage, v_b.*

through D_H fades to zero between S_L turn off and S_H turn on is D_L activated.

Starting with the S_H turn on current flows through it. When S_H is turned off current flows through D_L and S_L consecutively and, once the least is turned off, the current flows through D_H until it becomes zero, when the alternative diode activation state is reached.

Waveforms for the same power cases as in the previous subsection can be seen in Fig. 7.

As aforementioned, this asymmetrical strategy behaves as duty cycle modulation for high power output but for light-load operation present some advantages such as reduced current during S_H turn-on and more evenly shared power losses.

In addition, both strategies can be used complementary in order to take advantage of the benefits of each of them. This way, it is possible to balance power losses among the transistors and improve current consumption.

IV. Experimental Results

A prototype converter was implemented to validate the simulation results (Fig. 8). The experimental setup supplies two oval-shaped inductors, each connected to a half-bridge inverter.

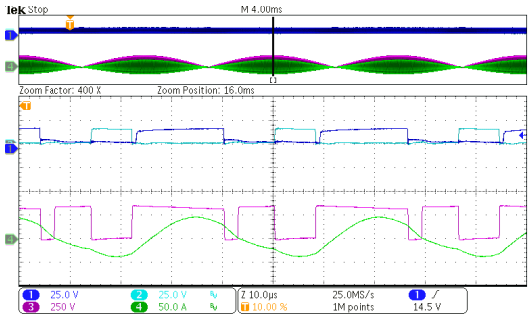

(a)

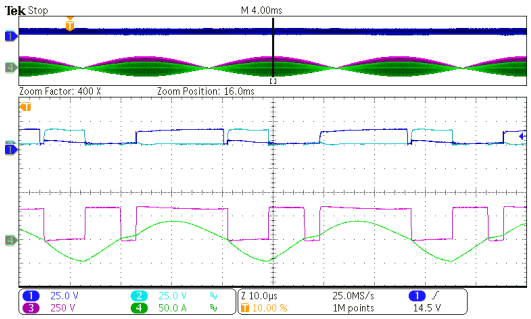

(b)

Fig. 9. *Experimental waveforms showing non-complementary pulse delay control (NC PDC) with α=100° (a) and non-complementary pulse width modulation (NC PWM) with φ=80° (b) asymmetrical stretegies used on 50% covered inductors. On each capture, from top to bottom: S_H gate voltage, $v_{SH,1}$, (25 V/div, dark blue), S_L gate voltage, $v_{SL,1}$, (25 V/div, cyan), Load 1 output voltage, $v_{o,1}$, (250 V/div, pink), Load 1 inductor current, $i_{o,1}$, (50 A/div, green). Time axis: 50 µs/div.*

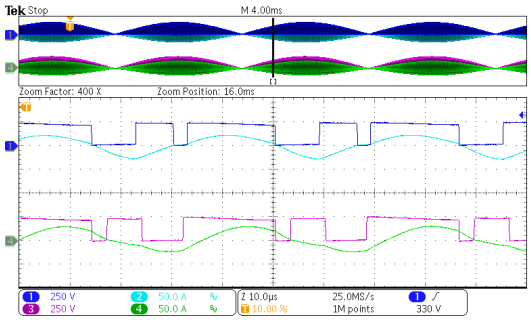

Fig. 10. *Experimental waveforms showing both asymmetrical stretegies simultaneously used on 50% covered inductors, 1000 W per load, α=100°, φ=80°. From top to bottom: Load 1 output voltage, $v_{o,1}$, (250 V/div, dark blue), Load 1 inductor current, $i_{o,1}$, (50 A/div, cyan), Load 2 output voltage, $v_{o,2}$, (250 V/div, pink), Load 2 inductor current, $i_{o,2}$, (50 A/div, green). Time axis: 50 µs/div.*

Fig. 9 shows the experimental waveforms for the proposed control strategies, including control signals, the output voltage, v_o, and current through the load, i_o. Fig. 9 (a) shows the half bridge operating with the NC PDC strategy and Fig. 9 (b) shows the NC PWM strategy for the simulated case.

Additionally, Fig. 10 shows power strategies independence by applying each of them simultaneously to reach an output power of 1000 W. In addition, power curves have been

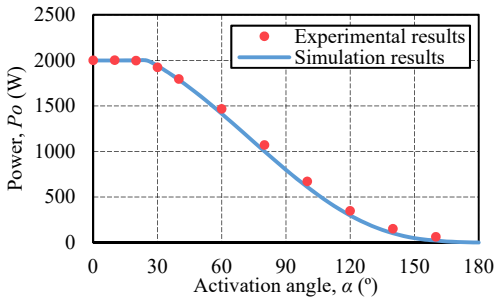

(a)

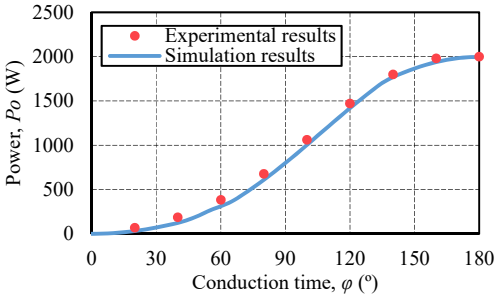

(b)

Fig. 11. *Power curves for different activation angle, α, variation in NC PWM strategy (a) and conduction time, φ, variation in NC PDC strategy (b) starting at 2000 W. Activation angle and conduction time in degrees with 360° as total switching period.*

generated for both proposed modulations, while providing objective power to the 100% covered inductor. In Fig. 11 (a) achieved power with the NC PDC strategy for a given frequency can be seen. It starts at a high power level and can be reduced to zero by increasing the activation angle. In Fig. 11 (b) achieved power with the NC PWM strategy can be seen. It starts at a high power level and can be reduced to zero by reducing the active time, φ.

V. Conclusions

In this paper, two asymmetrical conduction mode strategies have been presented in order to provide shared frequency independent power control for induction cooktops. The first is based on retarded low side transistor activation whereas the latter relies on anticipated deactivation of the transistor. Both achieve complete power control over the load while maintaining the switching frequency and can be used in combination to provide a better current consumption or balance power losses between the half bridge transistors.

The proposed strategies have been experimentally verified and compared with previous state-of-the-art modulation strategies. As a conclusion, the proposed asymmetrical modulation strategy based on anticipated low side transistor deactivation achieve reduced losses outperforming classical duty variation.

Acknowledgment

This work was partly supported by the Spanish MINECO under Project TEC2016-78358-R, by the Spanish MICINN and AEI under Project RTC-2017-5965-6, co-funded by EU through FEDER program, by the DGA-FSE, by the MECD under the FPU grant FPU17/01442, and by the BSH Home Appliances Group.

References

[1] O. Lucía, P. Maussion, E. Dede, and J. M. Burdío, "Induction heating technology and its applications: Past developments, current technology, and future challenges," *IEEE Transactions on Industrial Electronics,* vol. 61, pp. 2509-2520, May 2014.

[2] O. Lucía, J. Acero, C. Carretero, and J. M. Burdío, "Induction heating appliances: Towards more flexible cooking surfaces," *IEEE Industrial Electronics Magazine,* vol. 7, pp. 35-47, September 2013.

[3] H. Sarnago, L. Ó, and J. M. Burdío, "FPGA-Based Resonant Load Identification Technique for Flexible Induction Heating Appliances," *IEEE Transactions on Industrial Electronics,* vol. 65, pp. 9421-9428, 2018.

[4] J. Acero, C. Carretero, L. Ó, R. Alonso, and J. M. Burdío, "Mutual Impedance of Small Ring-Type Coils for Multiwinding Induction Heating Appliances," *IEEE Transactions on Power Electronics,* vol. 28, pp. 1025-1035, 2013.

[5] J. Acero, C. Carretero, I. Lope, R. Alonso, L. Ó, and J. M. Burdio, "Analysis of the Mutual Inductance of Planar-Lumped Inductive Power Transfer Systems," *IEEE Transactions on Industrial Electronics,* vol. 60, pp. 410-420, 2013.

[6] C. Carretero, O. Lucia, J. Acero, and J. M. Burdio, "Computational Modeling of Two Partly Coupled Coils Supplied by a Double Half-Bridge Resonant Inverter for Induction Heating Appliances," *IEEE Transactions on Industrial Electronics,* vol. 60, pp. 3092-3105, 2013.

[7] H. P. Ngoc, H. Fujita, K. Ozaki, and N. Uchida, "Phase Angle Control of High-Frequency Resonant Currents in a Multiple Inverter System for Zone-Control Induction Heating," *IEEE Transactions on Power Electronics,* vol. 26, pp. 3357-3366, 2011.

[8] F. Forest, S. Faucher, J. Gaspard, D. Montloup, J. Huselstein, and C. Joubert, "Frequency-Synchronized Resonant Converters for the Supply of Multiwinding Coils in Induction Cooking Appliances," *IEEE Transactions on Industrial Electronics,* vol. 54, pp. 441-452, 2007.

[9] I. Millan, J. M. Burdio, J. Acero, O. Lucia, and D. Palacios, "Resonant inverter topologies for three concentric planar windings applied to domestic induction heating," *Electronics Letters,* vol. 46, pp. 1225-1226, 2010.

[10] H. Sarnago, L. Ó, M. Pérez-Tarragona, and J. M. Burdío, "Dual-Output Boost Resonant Full-Bridge Topology and its Modulation Strategies for High-Performance Induction Heating Applications," *IEEE Transactions on Industrial Electronics,* vol. 63, pp. 3554-3561, 2016.

[11] O. Lucia, J. M. Burdio, I. Millan, J. Acero, and D. Puyal, "Load-Adaptive Control Algorithm of Half-Bridge Series Resonant Inverter for Domestic Induction Heating," *IEEE Transactions on Industrial Electronics,* vol. 56, pp. 3106-3116, 2009.

[12] Ó. Jiménez, O. Lucia, I. Urriza, L. A. Barragan, P. Mattavelli, and D. Boroyevich, "An FPGA-Based Gain-Scheduled Controller for Resonant Converters Applied to Induction Cooktops," *IEEE Transactions on Power Electronics,* vol. 29, pp. 2143-2152, 2014.

[13] Ó. Jiménez, Ó. Lucía, I. Urriza, L. A. Barragán, and D. Navarro, "Analysis and Implementation of FPGA-Based Online Parametric Identification Algorithms for Resonant Power Converters," *IEEE Transactions on Industrial Informatics,* vol. 10, pp. 1144-1153, 2014.

[14] O. Lucia, C. Carretero, D. Palacios, D. Valeau, and J. M. Burdio, "Configurable snubber network for efficiency optimisation of resonant converters applied to multi-load induction heating," *Electronics Letters,* vol. 47, pp. 989-991, 2011.

[15] H. Sarnago, L. Ó, A. Mediano, and J. M. Burdío, "Analytical Model of the Half-Bridge Series Resonant Inverter for Improved Power Conversion Efficiency and Performance," *IEEE Transactions on Power Electronics,* vol. 30, pp. 4128-4143, 2015.

[16] C. Carretero, O. Lucía, J. Acero, R. Alonso, and J. M. Burdío, "Frequency-dependent modeling of domestic induction heating systems using numerical methods for accurate time-domain simulation," *IET Power Electronics,* vol. 5, pp. 1291-1297, September 2012.

[17] O. Lucía, J. M. Burdío, I. Millán, J. Acero, and L. A. Barragán, "Efficiency oriented design of ZVS half-bridge series resonant inverter with variable frequency duty cycle control," *IEEE Transactions on Power Electronics,* vol. 25, pp. 1671-1674, July 2010.